



Italian Society
of Periodontology
and Implantology

Multi-layered chitosan-based construct and periodontal regeneration: functional layers for multi-tissue interface

Costrutto multi-strato in chitosano per la rigenerazione parodontale: strati funzionali per interfaccia multi-tissutale

Varoni E.M.¹, Xu J.¹, Cochis A.², Chin H.¹, Altomare L.⁴, Lodi G.³, De Nardo L.⁴, Quinn S.¹, Carrassi A.³, Rimondini L.², Cerruti M.¹

¹Department of Mining and Materials Engineering, Mc Gill University, Montreal, Canada

²Department of Health Sciences, Università del Piemonte Orientale, Italy

³Department of Biomedical, Surgical and Dental Sciences, Università degli Studi di Milano, Italy

⁴Department of Chemistry, Materials Sciences and Chemical Engineering "G. Natta", Politecnico di Milano, Milan, Italy

PROCEEDINGS BOOK RESEARCH SESSION "H.M. GOLDMAN PRIZE" 2013
ATTI DELLA SESSIONE DI RICERCA "PREMIO H.M. GOLDMAN" 2013

Summary

Aims: development of a multi-layered three-dimensional chitosan scaffold for multi-tissue periodontal regeneration, with fine-tuned structure and physical-chemical properties, according to the different periodontal parts to be regenerated, able to drive multi-tissue regeneration in harmony with the correct periodontal anatomy, to maintain the space for the development of different tissues, adaptable to bone defects, resorbable. **Materials and Methods:** we obtained and fully characterized a chitosan sponge-like and multi-layered scaffold, by cross-linking chitosan with genipin and lyophilization. It was composed by a low molecular weight (LMW) chitosan layer for mucosa interface, and a medium molecular weight (MMW) chitosan layer for bone. An oriented structure for periodontal ligament was developed by chitosan electrodeposition. **Results:** the two layers showed an highly porous cross-linked structure, with immediate hydration. Four-weeks degradation, in presence or not of lysozyme, was similar for both the layers, but MPM part showed a slight better stability at 2 weeks. Mechanical properties displayed an increased resistance to compression of MMW chitosan layer. Oriented pore structure was successfully produced. High cytocompatibility and no cytotoxicity were found by *in vitro* tests. **Conclusions:** the scaffold showed tunable structure and physical-mechanical properties, suggesting a promising approach for multi-tissue periodontal regeneration.

Riassunto

Scopo: sviluppare un costrutto multi-strato 3D da impiegare per la rigenerazione parodontale, dotato di proprietà fisico-meccaniche in sintonia con il tipo di tessuto da rigenerare, adattabile ai difetti ossei, riassorbibile, capace di guidare la rigenerazione multi-tissutale secondo la corretta anatomia parodontale, mantenendo lo spazio necessario allo sviluppo dei diversi tessuti. **Materiali e Metodi:** tramite reticolazione di chitosano con genipina e liofilizzazione, è stato ottenuto e caratterizzato un costrutto spugnoso, multistrato, con strato in chitosano a basso peso molecolare (BPM) all'interfaccia mucosa, a medio peso molecolare (MPM) all'interfaccia ossea.

È stata sviluppata struttura orientata per le fibre del legamento tramite elettrodeposizione di chitosano. Risultati: i due strati mostravano struttura reticolata porosa, rapidamente idratabile. La degradazione in vitro a 4 settimane, in presenza o meno di lisozima, era simile per entrambi gli strati, pur presentando lo strato a MPM una stabilità a 2 settimane migliore, seppur in modo non marcato. Le proprietà meccaniche evidenziavano maggior resistenza alla compressione della struttura a MPM. La porzione con pori orientati è stata sviluppata con successo. I test cellulari rivelavano elevata citocompatibilità ed nulla citotossicità. Conclusioni: il costrutto dimostra proprietà modulabili, per struttura e risposte fisico-meccaniche, suggerendo come possa essere adatto alla rigenerazione parodontale multi-tissutale.

Introduction

Periodontal apparatus is the complex multi-tissue system, anchoring the teeth in the maxillar/mandibular bone. It includes dental root cementum, periodontal ligament (collagen fibers), dento-gingival sulcus (epithelium and derma) and alveolar bone.

Chronic periodontitis is the inflammatory disease of this system, producing its desorption and representing one of the major global health problem. It afflicts about 20% of adults and nearly the 90% of elder population worldwide (Petersen and Baehni 2012). Severe functional and psycho-social consequences have been related to periodontal patients with influence on general health and impact on public health economy (Watt and Petersen 2012).

Regenerative periodontal therapy (RPT) has the ideal aim and the future challenge to reconstitute complete periodontal apparatus, restoring its architecture and function (Bossart and Sculean 2009). The obstacle to achieve periodontal regeneration after conventional mechanical treatment (scaling and root planing) is the proliferation of epithelial tissues into the defect at a faster rate than that of mesenchymal tissues. This leads to the formation of a long junctional epithelium, preventing the selective migration, proliferation and differentiation of cells derived from cementum, periodontal ligament and alveolar bone.

Two cornerstones can be identified in RPT.

The first is the stability of blood clot during the healing, which spatially and temporally drives the colonization of different tissue populations. Nowadays, three RPT techniques have been proposed, but only a portion of the defect can be successfully regenerated and different biomaterials proposed are related to potential complications which can compromise the success of the treatment (Bottino et al. 2012, Ge et al. 2012, Xu et al. 2012): 1) guided tissue regeneration (GTR), using resorbable or non resorbable as physical barriers to protect the clot and prevent soft tissue migration into periodontal defects, but exposition, contamination and collapse limit their usage; 2) guided bone regeneration for alveolar bone regeneration, using scaffolds or grafts; 3) biologically active regenerative materials which exploits molecules involved in physiological tooth development to regenerate the whole periodontium.

Recent research is now focused on reducing GTR complications and on regenerating those defects, wide and lacking of retentive bone walls, highly associated to clot instability.

The second aspect is ligament fiber orientation and integration with surrounding tissues (bone and cementum), to restore physiological function of ligament, mediating dento-alveolar adaptive response to mechanical stimuli (Park et al. 2010).

To date, multi-tissue spatial fibrous tissue organization and functional complete *restitution ad integrum*, using a single scaffold system remains a noteworthy challenge.

Therefore, the multi-layered scaffold here proposed wants to face these two aspects: 1) to obtain a precise anatomic scaffold, with specialized architecture and specific surface topography towards bone, mucosa and ligament sides, to regenerate soft/hard tissue compartments even in absence of a retentive bone defect; 2) to establish a 3D oriented pattern toward ligament, to drive its directionality (Fig. 1).

For these purposes, the scaffold is based on chitosan and genipin natural molecules. Chitosan (CH) is a polysaccharide, usually derived from crustaceans chitin: low cost, biodegradable, biocompatible, non-antigenic, non-toxic, biofunctional (Xu et al. 2011), adhesive, haemostatic and antibacterial, wound healing accelerator (Francesco and Tzanov, 2011; Tchemtchoua et al., 2011). Mechanical and biological properties can be potentially tunable on molecular weight (high, medium or low) and/or degree of acetylation (Kim et al. 2008, Zunying et al. 2012). Moreover, two further aspects of CH are desirable in the development of RPT device, i.e. its considerable antibacterial activity against a broad spectrum of bacteria (Kim et al. 2008) and its bio-adhesivity (Bonferoni et al. 2009), both useful in wound healing and in decreasing the possibility of scaffold exposition and contamination.

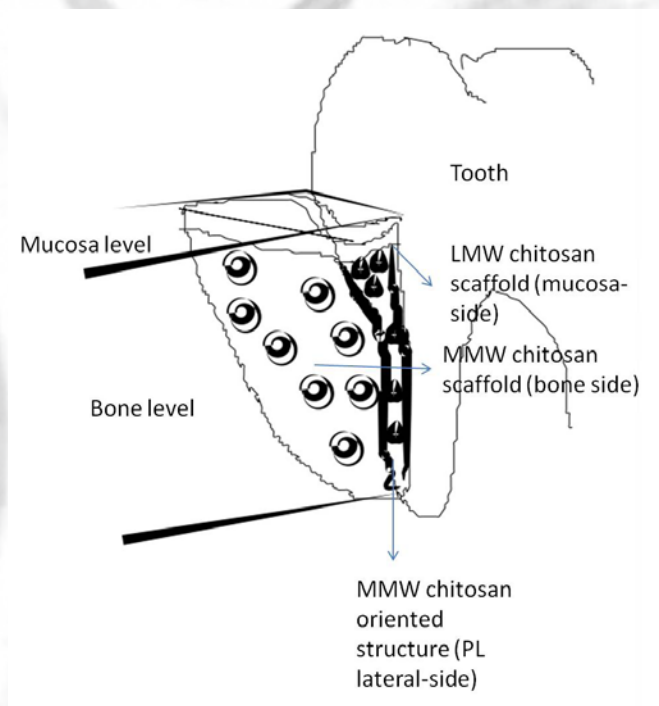
CH polymerization leads to the formation of film and porous scaffold, but with rapid biodegradation and low mechanical responses (Kim et al. 2008; Muzzarelli 2009). To improve this aspect, genipin, an aglycone geniposide extracted from the fruits of *Gardenia jasminoides Ellis*, is commonly used to reinforce CH structural stability, as biocompatible cross-linking agent (Muzzarelli 2009; Wang et al. 2011).

Recently, CH cross-linked with genipin has been proposed as biomaterial for skin, bone and periodontal regeneration (Kim et al. 2008, Xu et al. 2011).

Thus, based on CH-genipin scaffold, we obtained and characterized a novel multi-layered device, with fine-tunable architecture, in the perspective of producing a multi-tissue regenerative tool.

Figure 1. Structure of multi-layered scaffold.

- “Bone-side”. A lower thick layer, for alveolar bone regeneration, will be made of a porous and stiff scaffold, as space maintainer, even in presence of wide defects.
- “Mucosa-side”. An upper thin layer, for the interface with gingiva, will be made of a dense and porous scaffold, cross-linked with 0.1% of genipin, positioned on MMW layer, to hinder epithelial cell colonization of bone compartment, promoting gingival healing.
- “Lateral-side” fiber-guiding scaffold structure for periodontal ligament (PL). Oriented structure, on the lateral side of the scaffold toward the dental root, will be deposited to reproduce periodontal space. The pore net will support periodontal ligament (PL) fibroblasts to penetrate and produce oriented fibers, perpendicularly to dental root.



Materials and Methods

Synthesis and physical-chemical characterization.

Bone and mucosa compartments. A bi-layered scaffold was manufactured by subsequently

pouring two CH hydrogels, low molecular weight (LMW) and medium molecular weight (MMW) respectively, on each other, as follows:

- 1. “*Bone-side*”. “*Bone-side*”. Synthesis of 2% MMW CH gel, cross-linked with 0.1% of genipin, for bone regeneration.

- 2. “*Mucosa-side*”. Synthesis of 2% LMW CH gel, cross-linked with 0.1% of genipin, positioned on MMW layer, for gingival interface.

Briefly, single and double layers were produced from a starting solution containing 2 % of CH prepared by dissolving CH powder in distilled water, 1% acetic acid, at RT. Genipin powder was dissolved in ethanol and added to CH solution to a final concentration of 0.1% (Moura et al. 2011). For mono-layer scaffold (both LMW or MMW), a 3ml-volume of solution was poured and cured for 12h at 37°C, then for 24h at room temperature, till gelification.

For bi-layer scaffold, a 2 ml-volume of MMW CH solution was poured at first. After 12 h of curing at RT, the second 1ml-volume of LMW CH solution was poured on the top of the first gel and cured again for 4 h at 37°C, then 24 h at RT.

All constructs were freeze-dried.

Structure morphology was ascertained by Scanning Electron Microscopy (SEM).

Oriented structure compartment for periodontal ligament. CH film with oriented pores was obtained by cathodic electro-deposition (Altomare et al. 2012). Morphology and thickness were observed by stereo-microscope and SEM.

LMW vs MMW CH single scaffolds. Mono-layer scaffolds were used for comparisons. Characterization was repeated in triplicate.

- *Ninhydrin assay* (Moura et al. 2011) investigates cross-linking degree, determining the percentage of free amino groups of the CH scaffolds, after the cross-linking reaction. About 3 mg of each lyophilized sample was heated for 20 min to 100° C in a water bath, with 500 ul of the ninhydrin solution. After cooling at RT, solution optical absorbance (Abs) was determined at 570 nm by UV-Vis spectrophotometer. For standard curve calculation, CH solution, at different concentrations, was used. The following equation was applied: degree of cross-linking (%)= [(Abs CH powder– Abs CH scaffold) / Abs CH powder]*100

- *Swelling tests* (Moura et al. 2011) were performed on the CH scaffolds after lyophilization. After preliminary dried weight analysis (Wd), they were incubated in PBS (pH 7.4) at 37 C° for 24 h to reach their equilibrium water content state. At different times, the excess of incubating medium was gently removed and samples weighed (We). The equilibrium water content (EWC) was calculated as: EWC (%)= [(We-Wd)/We]*100

- *In vitro degradation* (Moura et al. 2011) was investigated by comparing the presence or not of lysozyme. The weight of the dried scaffolds (Wi) was monitored as a function of the incubation time (up to 4 weeks) in 1 ml of PBS at 37°C. Concentration of lysozyme was chosen to correspond to that in human serum (1.5 µg of lysozyme/ml), and refreshed each day to physiological conditions. At specified time intervals, scaffolds were lyophilized and weighed (Wt). The extent of *in vitro* degradation was expressed as: Weight loss (%)= [(Wi – Wt)/Wi]*100

- *Mechanical Properties* (Thein-Han and Misra 2009). Confined compression modulus *HA* was measured as previously described (Chin et. 2011): a 3mm-samples (both LMW and MMW) were subjected to confined compression at 15%, 20%, and 25% of the free swelling thickness. *HA* was then determined from the plot of equilibrium stress versus strain.

Biological characterization.

Scaffolds were previously immersed in 100% and 50% ethanol solutions (1h each) for sterilization, then rinsed with PBS. Experiments were performed 6 times for controls and each different samples.

Cell cultures. MG63 cells (human osteosarcoma cell line) were maintained at 37C° under 5% CO₂, in DMEM supplemented with 10% FBS, penicillin (100 U/cm³), and streptomycin (100 µg/

cm³). Primary human gingival (hG) fibroblasts and primary human (hPDL) periodontal ligament fibroblasts were isolated from gingival biopsies and from ligament of a pool of extracted teeth, respectively. The tissues were digested 45 min at 37°C with a solution of 1% Type I collagenase, 0.1% proteinase and 25% trypsin in a serum free minimal essential medium alpha modification (α -MEM). Afterwards, digested solution was filtered with 0.45mm filters in order to remove undigested debris and centrifuged 10 minutes at 800 rpm. The pellet was then re-suspended in α -MEM plus 10% FBS, 1% antibiotics/antimycotics (penicillin/streptomycin/gentamycin) and plated into new polystyrene Petri plates. Cells attached to the polystyrene surface after about 12 hours, while the correct morphology was observed after 48 hours. Cells from passage 2 to 5 were used for experiments.

Cell viability.

- *Cytocompatibility.* For the direct contact assay, cells were seeded in a defined number directly onto the surfaces of each samples (both mono-layer and bi-layer scaffolds). Cells viability was evaluated after 72h with the (3-(4,5-Dimethylthiazol-2-yl)-2,5-diphenyltetrazolium bromide colorimetric assay (MTT). Briefly, 100ul of MTT solution (3mg/ml in phosphate buffered saline (PBS), ph 7.4) were added to each sample and incubated 4 hours in the dark; afterwards, formazan crystals were solved with 100ul of dimethyl sulphoxyde and 50 ul were collected. Surnatant optical density (o.d.) was evaluated at 570nm with a spectrophotometer. Plastic well was considered as 100% cells viability, samples viability was calculated as follow: (sample o.d. / control o.d.)*100.

- *Cytotoxicity.* For the indirect assay, serum free α -MEM was incubated without cells for 1 week at 37°C, 5% CO₂ in direct contact with samples (both mono-layer and bi-layer scaffolds). Afterwards, eluates were collected, added with 10% FBS and used to cultivate cells. Cells were seeded in a defined number and cultivated for 1 week at 37°C, 5% CO₂. Afterwards, cells viability was evaluated by the MTT test as previously described.

- *Cell morphology.* Cell morphology was investigated using Scanning Electron Microscopy (SEM), after fixation with 2,5% glutaraldehyde in 1 mol/L sodium cacodylate buffer for 2 hours, specimens were dehydrated in ethanol and, finally, freeze-dried.

Statistical analysis.

Mean values were calculated, together with Standard Deviation. Student's t test was used to compare two different means, significance level was considered for $p < 0.05$.

Results

Synthesis and physical chemical characterization.

Bi-layered scaffold. SEM images (Fig. 2, A and B) describe the bi-layered scaffold at the interface between porous MMW and LMW CH compartments. The MMW sponge-like scaffold displayed a porosity of about 150 μ m in diameter. The LMW layer showed a dense structure with pore dimension of about 50 μ m. The two layers appeared well adhered to each other.

Oriented Pore Structure. Self-standing oriented pore net was successfully obtained. The macroporosity (Fig. 3A) was of about 450 μ m in diameter. A random micro-porosity (Fig. 3B) can also be observed, with a pore dimension of about 20 μ m, probably related to hydrogen bubble release for water electrolysis, consequently entrapped in the CH gel during electro-deposition (Simchi et al. 2009). The thickness of the layer was about 250 μ m, similar to human periodontal biological space (Bosshardt and Sculean 2009). This oriented pattern will have the function to promote PDL fibroblasts to penetrate and produce selectively and functionally oriented PDL fibers, perpendicularly to dental root, as already proposed by Park and colleagues (Park et al. 2011).

LMW vs MMW CH single scaffolds. Porous structure of the single layers was confirmed using SEM (data not shown).

- *Ninhydrin assay,* evaluating the amount of scaffold free amino groups, revealed a cross-linking

degree of 32.22 ± 19.43 % for MMW CH scaffolds, of 24.38 ± 14.63 % for LMW CH scaffolds. This data are consistent with FT-Infrared spectroscopy, which showed the presence of genipin in the scaffolds, with a peak centered around 1700 cm^{-1} , attributed to the C=O stretching of genipin molecule (data not shown).

- *Swelling measurement*, as water content at equilibrium (Fig. 4A), revealed as the scaffold was quickly and efficiently imbibed by the liquid, soon after 5 min of hydration. EWC mean values were: $89.49\% \pm 0.39$ and $89.5\% \pm 0.6$ for MMW and LMW CH scaffold, respectively. This result confirms a sponge-like structure of the scaffold, suggesting the facility of be colonized by liquid and, in perspective, by clot.

- *In vitro degradation test* showed a slow and constant degradation of the scaffold during the time (Fig. 4B). For MMW CH scaffold, the final weight loss, at 4 weeks, was of $35.45\% \pm 4.45$ in presence of lysozyme, while of $28.67\% \pm 0.97$ in absence of enzyme. For LMW CH scaffold, the final weight loss, at 4 weeks, was of $40.45\% \pm 1.79$ in presence of lysozyme, of $34.03\% \pm 1.37$ in absence. As expected the former scaffold was associated to a slight lower degree of degradation, possibly related to a slightly higher cross-linking degree, as previously described, and/or related to the higher MW, which corresponds to longer polymer chains to be degraded. In particular, MMW CH appeared more stable than LMW CH scaffold at second week in PBS, suggesting a certain fine-tunable early degradability, which is crucial for clot retention and tissue regeneration. Indeed, the mucosa healing is biologically faster than bone healing: while they gradually degraded, they can be replaced by *situ*-specific new tissues. As Kim et al. reported, when a scaffold is used for bone tissue engineering, its degradation need to be quite slow, to maintain mechanical properties till tissue complete restoration (Kim et al. 2008). Thus, the two compartments of the bi-layered scaffold may finely support bone and mucosa tissue regeneration, respectively, and be degraded.

- *Mechanical tests* (Fig.5) showed a confined compression modulus (HA) of 51.9 ± 19.7 kPa and 24.3 ± 4.4 kPa, for MMW and LMW CH scaffold, respectively. These results suggest an higher stiffness of the former ($p < 0.05$, $p = 0.0271$), in accordance with a previous study, which correlates CH MW and increasing of compression modulus (Thien-Han et al. 2011). In addition, this finding further corroborates MMW CH potentiality in sustaining the upper LMW CH part and the blood clot, even in absence of retentive bone walls. On the other hand, a “softer” and adaptable LMW CH layer towards mucosa may allow a lower area of traction, decreasing the possibility of scaffold exposition. The fine-tunable mechanical properties of the structure, according to the different parts to be regenerated, can be observed, being, in term of resistance to compression, the MMW CH layer more similar to hard tissue as bone, while LMW CH more similar to soft tissue as mucosa (Misch et al. 1999, Lacoste-Ferrè et al. 2011).

Figure 2. SEM images of bi-layered scaffold. A- A dense and thin porous LMW CH layer can be observed (left), adhering to MMW CH sponge-like thicker layer (right). B- At the interface (arrow), compenetration between LMW CH layer (left) and MMW CH layer (right) can be observed.

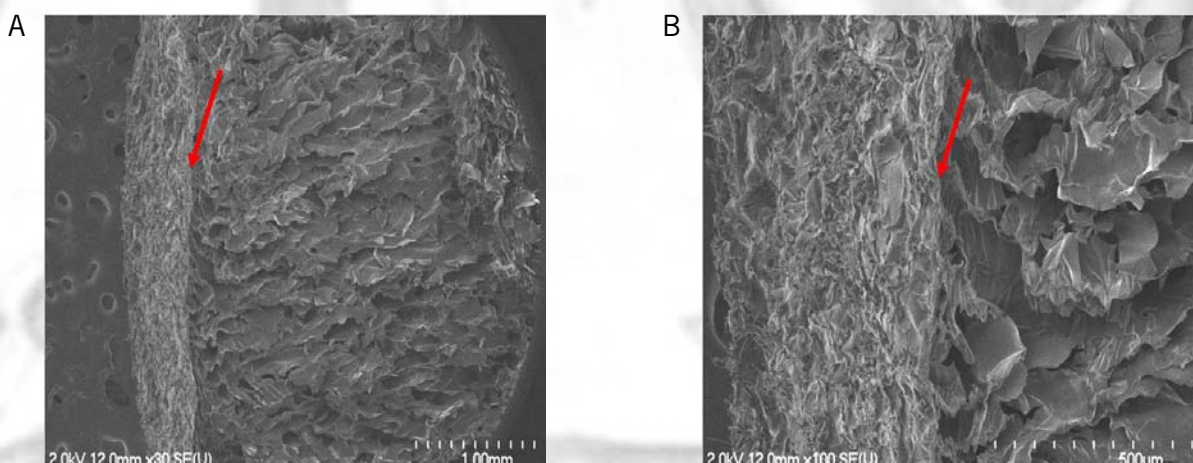


Figure 3. SEM image of oriented pore structure. The electrodeposited CH net displays an oriented macro-porosity, related to mesh, of about 450 μm in pore diameter (A), while a random micro-porosity, related to hydrogen entrapment, of about 20 μm (B).

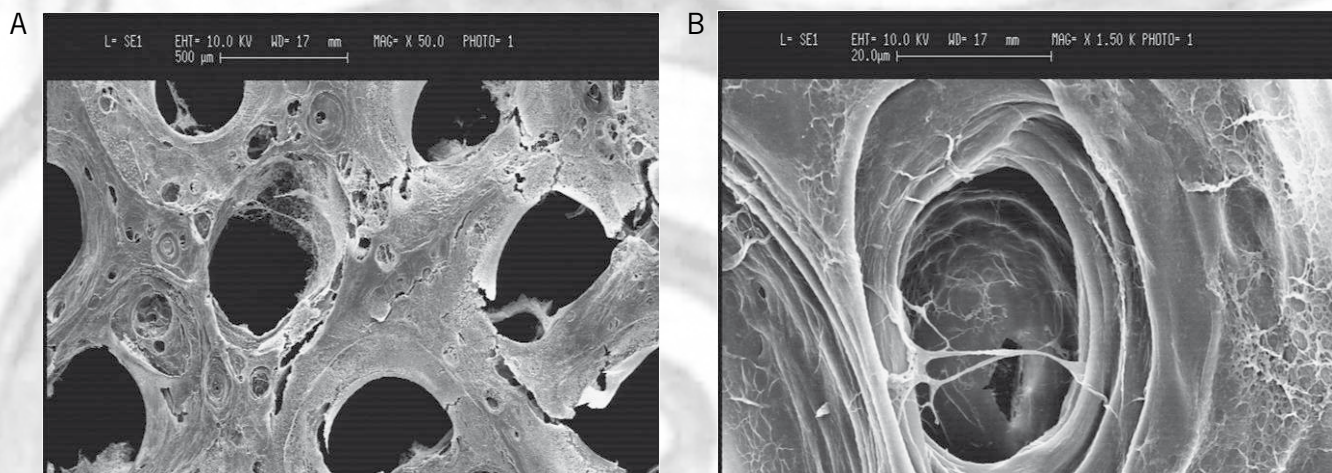


Figure 4. A- Swelling assay. Scaffold water content at equilibrium reveals high ability to be imbibed by a liquid (about 89% of EWC). A similar behaviour can be detected with LMW and MMW CH scaffold. B- In vitro degradation. The comparison of weight loss profiles of CH scaffolds, in PBS without or with lysozyme at 37° C, shows a slightly better stability of MMW CH scaffold, at least at 2 weeks. Points represent means \pm standard deviations.

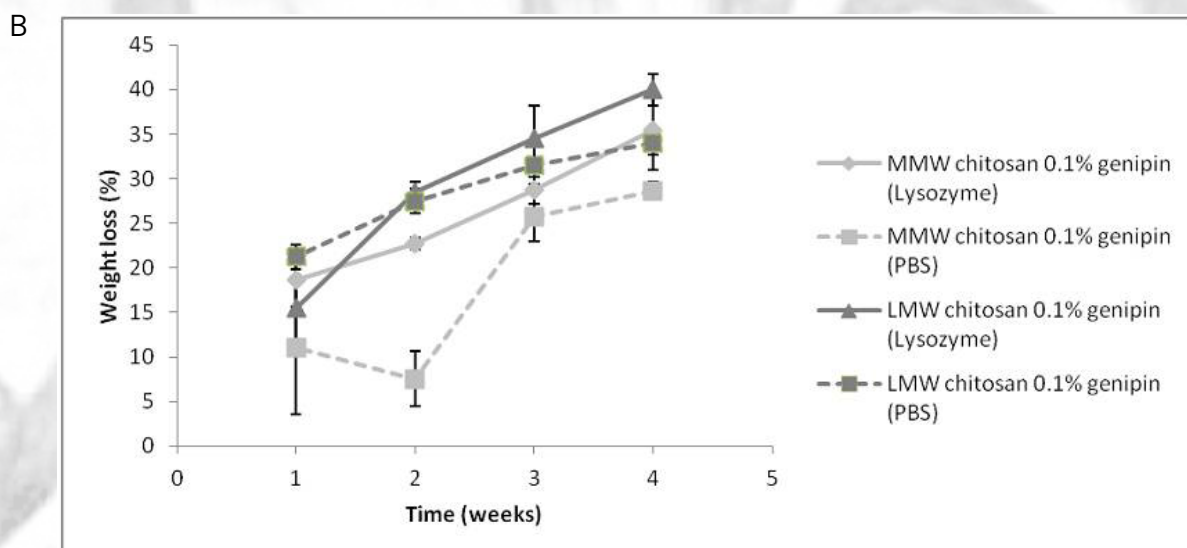
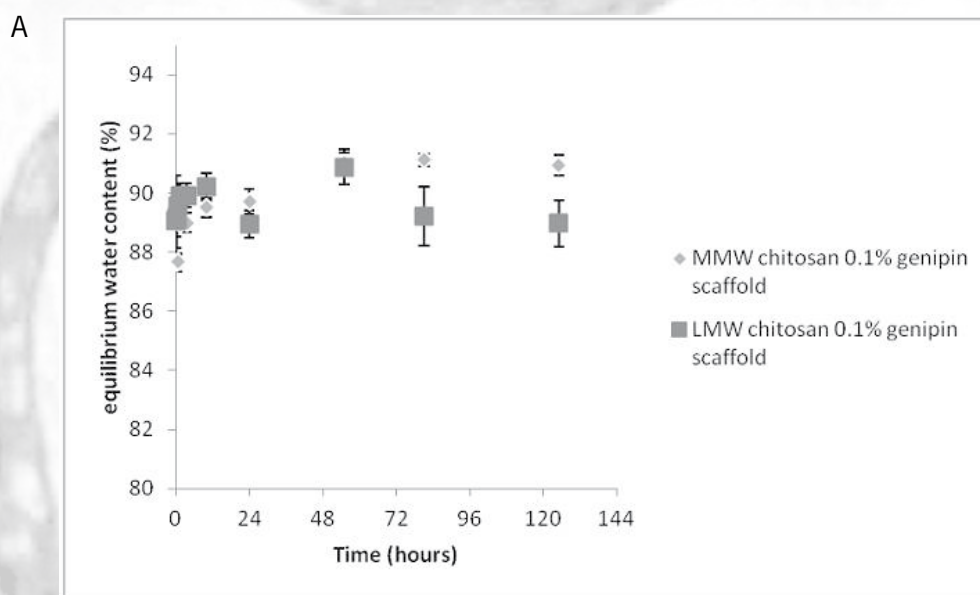
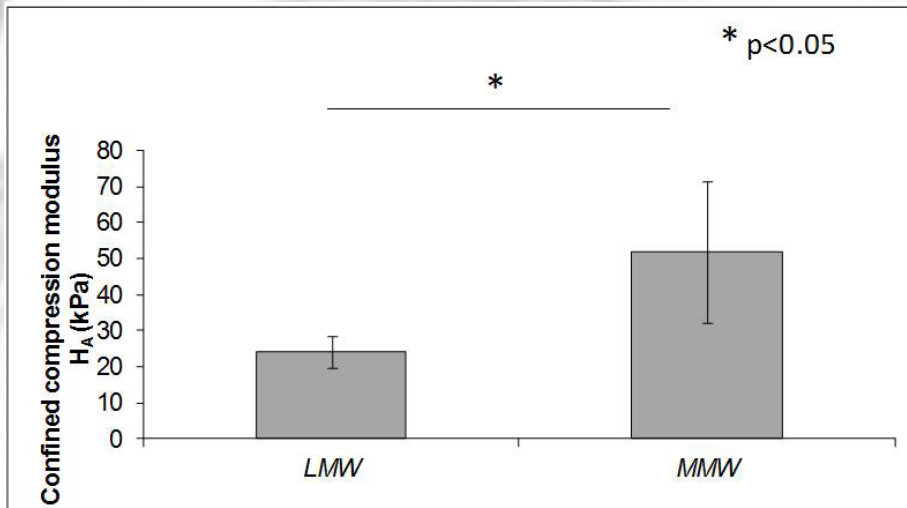


Figure 5. The comparison of the confined compression modulus (H_A), between LMW and MMW CH scaffolds highlights the increase in compression resistance with the increase of CH molecular weight. Bar represents mean value and standard deviation



Biological characterization.

Cell viability.

- *Cytocompatibility test* (Fig. 6A) demonstrated that cells cultivated directly on sample surface are able to successfully adhere and spread. Cells viability was similar to controls.

- *Cytotoxicity* (Fig. 6B). Viability of the cells was not significantly affected upon incubation with each of the scaffold extraction media used, suggesting that no toxic molecules were released into the medium by the samples, during the incubation period.

Cell morphology. MTT assays results were confirmed by observation of cells morphology at SEM. Figure 7 described hPDL fibroblasts after the seeding on MMW CH mono-layer scaffold.

These data are consistent with those reported in literature (Moura et al. 2011, Wang et al. 2011), confirming the biocompatibility of material proposed. Noteworthy, in this work we used periodontal-specific primary cells, i.e. fibroblasts isolated from human gingiva to test LMW CH mono-layer and the LMW bi-layer surface (mucosa interface), while fibroblasts isolated from human PDL to test MMW CH mono-layer and the MMW bi-layer surface (bone-PDL interface). Furthermore, the “bone-side” MMW CH scaffold was also evaluated using MG63 human osteosarcoma cells, considered a model for cell viability assays in bone tissue engineering (Shirosaki et al. 2005).

Figure 6. Cytocompatibility (A) and cytotoxicity (B) assay results. Bars represent means and standard deviations. Both test results show that the different scaffolds were not toxic for cells, nor in direct contact or in indirect contact, using the eluates derived from samples immersion as culturing media (hG fibroblasts= human gingival fibroblasts, hPDL fibroblasts= human periodontal ligament fibroblasts)

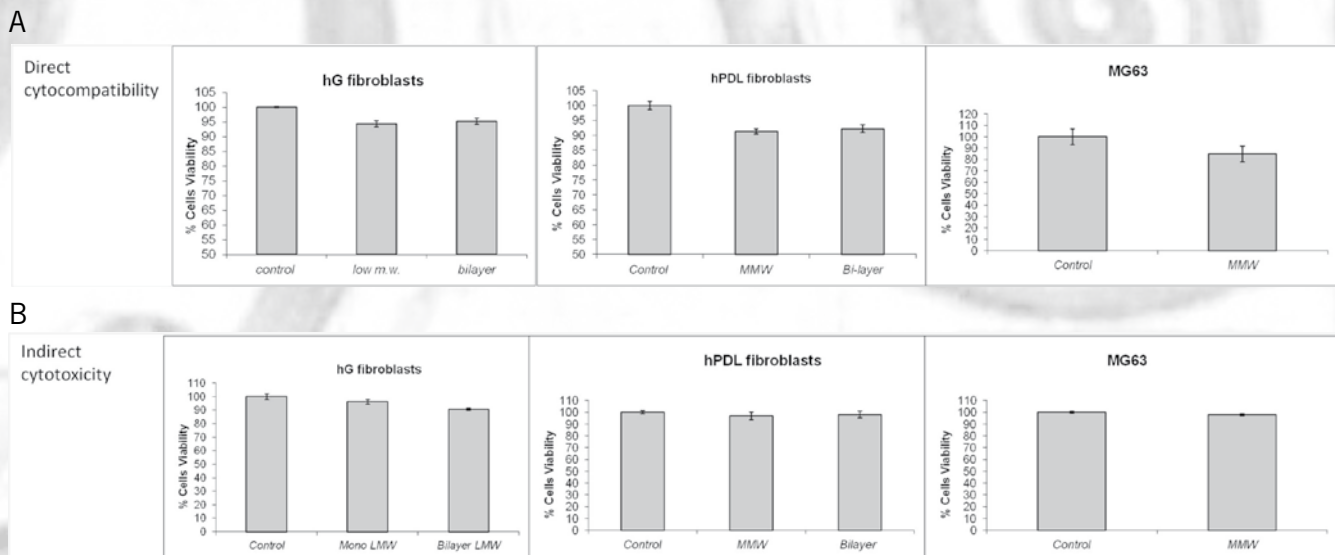
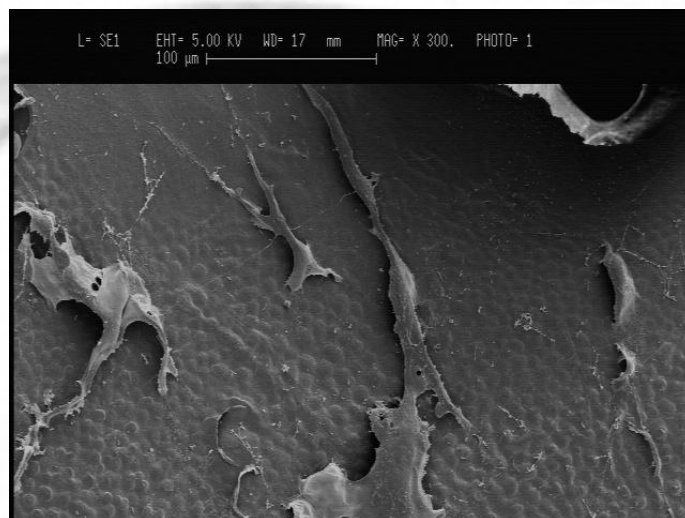


Figure 7. SEM morphological analysis of human periodontal ligament fibroblasts, after the seeding on MMW CH scaffold



Conclusions

The structure here proposed is a 3D biocompatible, sponge-like, resorbable, multi-layered scaffold. It displays fine-tuned physical properties, in harmony to the different periodontal parts to be regenerated.

The innovative oriented structure, with the aim of promoting ligament fibers organization, is a promising tool to further characterize. Future studies are also needed to investigate *in vivo* periodontal regeneration.

This scaffold appears a good candidate for multi-tissue engineering device. The final perspective is its application to different periodontal defects, in particular for those more difficult to treat, obtaining complete and stable periodontal regeneration and reducing intra/post-operative complications.

References

- Petersen and Baehni. Periodontal health and global public health. *Periodontol 2000* 2012 60:7-14
- Watt and Petersen. Periodontal health through public health-the case for oral health promotion. *Periodontol 2000* 2012 60:147-55.
- Bosshardt and Sculean. Does periodontal tissue regeneration really work? *Periodontol 2000* 2009 51:208-19
- Bottino et al. Recent advances in the development of GTR/GBR membranes for periodontal regeneration-A materials perspective. *Dent Mater* 2012 28:703-21
- Xu et al. Chitosan as a barrier membrane material in periodontal regeneration. *J Biomed Mater Res Part B* 2012 100B:1435-43
- Tchemtchoua et al. Development of a chitosan nanofibrillar scaffold for skin repair and regeneration. *Biomacromolecules* 2011 12:3194-204.
- Francesko and Tzanov. Chitin, chitosan and derivatives for wound healing and tissue engineering. *Adv Biochem Eng Biotechnol* 2011 125:1-27.
- Kim et al. Chitosan and its derivatives for tissue engineering applications. *Biotechnol Adv* 2008 26:1-21.
- Zunying et al. Effects of chitosan molecular weight and degree of deacetylation on the properties of gelatine-based films. *Food Hydrocolloids* 2012 26:311-317.
- Wang et al. Cytocompatibility study of a natural biomaterial crosslinker-Genipin with therapeutic model cells. *J Biomed Mater Res Part B* 2011 97B:58-65.
- Muzzarelli R. Genipin-crosslinked chitosan hydrogels as biomedical and pharmaceutical aids. *Carbohydrate Polymers* 2009 77: 1-9.
- Ge et al. Bone repair by periodontal ligament stem cell-seeded nanohydroxyapatite-chitosan scaffold. *Int J Nanomed* 2012 7:5405-14.
- Park et al. Biomimetic Hybrid Scaffold for Engineering Human Tooth-Ligament Interfaces. *Biomaterials* 2010 31:5945-52.

- Park et al. Tissue engineering bone-ligament complexes using fiber-guiding scaffolds. *Biomaterials* 2012 33:137-45
- Bonferoni et al. Chitosan and Its Salts for Mucosal and Transmucosal Delivery. *Expert Opin Drug Deliv* 2009 6:923-939.
- Altomare et al. Morphology tuning of chitosan films via electrochemical deposition. *Material Letters* 2012 78:18-21.
- Moura et al. In Situ Forming Chitosan Hydrogels Prepared via Ionic/Covalent Co-Cross-Linking. *Biomacromolecules* 2011 12:3275-84.
- Chin et al. Improved characterization of cartilage mechanical properties using a combination of stress relaxation and creep. *J Biomech* 2011 44:198-201.
- Simchi et al. Electrophoretic deposition of chitosan. *Material letters* 2009 63: 2253-56.
- Misch et al. Mechanical properties of trabecular bone in the human mandible: implications for dental implant treatment planning and surgical placement. *J Oral Maxillofac Surg* 1999 57:700-6.
- Lacoste-Ferré et al. Dynamic mechanical properties of oral mucosa: Comparison with polymeric soft denture liners. *J Mech Behav Biomed Mater* 2011 4:269-74.
- Shirosaki et al. *In vitro* cytocompatibility of MG63 cells on chitosan-organosiloxane hybrid membranes. *Biomaterials* 2005 26:485-93.

Corresponding Author:

Elena Maria Varoni, DDS, PhD,
Post-Doc Researcher at McGill University of Montreal (Canada)
Dept. of Mining and Materials Engineering
McGill University (Canada)